

## Improving the detection of excessive activation of ciliaris muscle by clustering thermal images

by B. Harangi\*, B. Nagy\* and A. Hajdu\*

\*University of Debrecen, Faculty of Informatics, POB 12, 4010 Debrecen, Hungary  
 {harangi.balazs, nagy.brigitta, hajdu.andras}@inf.unideb.hu

### Abstract

In this paper, we introduce a novel approach to detect the excessive activation of ciliaris muscle on thermal images. We examine the ciliaris muscle of the human eye which is responsible for bending the eye lens. We screen the malfunction (excessive activation) of this muscle which can be recognized by analyzing thermal images instead of an invasive and unpleasant regular clinical procedure. The detection is based on eye region localization on a thermal image, statistical features extraction from the localized regions and a classification step with an optimal adjusted SVM classifier. To further improve the sensitivity and specificity of our method, we divide the images into clusters with k-means clustering based on the histogram of the images; and determine optimal parameter setup of the SVM classifier for each cluster. As the presented experimental results show, this approach is very promising, and the clustering of thermal images indeed leads to an improvement.

### 1. Introduction

The ciliaris muscle is a ring shaped striated muscle which surrounds the crystalline lens in the middle layer of the eye as can be seen in Figure 1. This muscle partly responses for the accommodation of the eye for viewing object at different distance. In other words, this muscle contracts when someone looks at a close object and relaxes when someone looks far. So when this muscle is in tension, it causes the lens to become more spherical and the eye can compose sharp picture of close objects and when it is relaxed, the eye can unbend and see sharply the far objects.

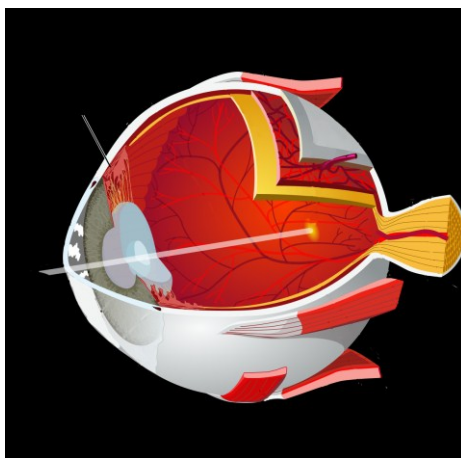


**Fig. 1.** Model of the human eye and the location of the ciliaris muscle.

In case of stress, long-term reading or frequent work with computers, the muscle cannot relax, thus, the tension of the muscle becomes permanent causing difficulties in long range focus and far sight may also become obscure. In this case, the eye tries to correct this inappropriate bending but the persistent cramp status of this muscle may lead to e.g. a regular head-ache. Furthermore, the regularly applied non-invasive refractometer analyzing of the eye is not able to detect this abnormal influence of this muscle. As a usual clinical mistake, improper dioptre adjustment is determined to correct this inappropriate bending of the eye while cramp status of the ciliaris muscle causes further unpleasant affects e.g. common eye-tiredness. After the improper dioptre wearing, the activity of this muscle will be suspected and this case the muscle can be disabled with a certain eye drop. However, this eye drop is not applied routinely because it is rather demanding with ruining the sharp sight during the investigation.

Sight problems occur in a very wide range within the human population because of the growing usage of computers. To help with the problem, our aim is to develop an alternative method to detect the malfunction of the ciliaris muscle under the regular examination of the eye without applying the demanding eye-drop based investigation. Such an alternative method can assist to the proper adjustment of the eye and shorten of the process of the adjustment.

Since the ciliaris muscle is close to the exterior surface of the eye, we have the opportunity to take advantage of thermal monitoring of it. The main line of the research is to detect the extra quantity of heat stemming from the excessive

activity of the ciliaris muscle which appears at special areas of the eye. The larger activity of the muscle is proportional to the higher temperature observed in these regions of the eye.

In our former work [1], we have taken the first steps towards the detection of the excessive activation of ciliaris muscle on thermal images. We proposed a basic method to label the images as “excessive activation/non- excessive activation” based on some simple statistical descriptors of the temperature distribution of the eye region. Now, we propose a novel approach to improve the accuracy of our detection method by clustering image databases, since they usually contain images with different characteristics such as different average temperature of the patients. For each cluster, an optimal parameter setting is determined for extracted feature selection and for the classifier used for image labeling. Since the data is represented in a more detailed form after clustering, we can expect a natural improvement that expectations we could validate by our experimental studies.

The rest of this paper is organized as follows: in section 2, we give an overview about our statistical feature extraction method, whose output is needed for the classifier. Section 3 describes our image clustering approach, while we explain the selection of the optimal parameters for the classifier for each cluster in section 4. We present our experimental results in section 5. Finally, we draw some conclusions in section 6.

## 2. Feature extraction based on temperature value statistics

To classify thermal images, first we execute a normalization step on each of them. In this normalization step, we assign new value for each pixel according to the following formulas:

$$x_{i_{new}} = \frac{x_i - \mu}{\sigma}, \text{ where } \mu = \frac{1}{N} \left( \sum_{i=1}^N x_i \right), \sigma = \sqrt{\frac{1}{N} \left( \sum_{i=1}^N x_i - \mu \right)},$$

where  $x_i$  is the intensity value calculated as the measured temperature at the  $i^{th}$  image point and  $N$  is the number of the total points in the head silhouette of the patient. It is possible that two images have similar intensity distributions. However, this step is necessary for normalization, since the temperature of the tissues of the patient depends on the average internal temperature of the body, but also on the temperature of the examination room. For the appropriate operation of the classifier, the input images to be classified should be similar to the training images. To enhance the performance of the system, we propose image database clustering instead of normalization.

Since the location of the ciliaris muscle is 1-2 mms away in both directions from the edge of the cornea, the examination of these special points would be sufficient. However, thermal images do not contain sufficient spatial information and sharp edges. Therefore, we cannot localize these points correctly. Thus, an elliptical region is selected manually to cover the eye, which is automatically divided into sub-regions from which we retrieve the following statistical descriptors: mean, variance, skewness, kurtosis, energy and entropy of the intensity histogram of the sub-regions, entropy, energy, contrast, homogeneity, mean, standard deviation, correlation, maximal probability, inverse difference of gray-scale co-occurrence matrix of the sub-regions according to the related literature [2-3]. So, we extract these first- and second-order statistical descriptors to create feature vectors for the classification algorithms. As classifier, we used support vector machines (SVM) to decide whether the input image should be considered as normal or abnormal.

## 3. Image database clustering

In this section, we present our image database clustering approach. To improve accuracy of the classification, we divide the images into three disjoint sets. The aim of this step is to resolve the variances among images caused by different temperature conditions at acquiring them. The image clustering provides separability of the lower temperature bodies from the higher temperature ones. Note that, the lower temperature image class is expected to contain less abnormal cases.

### 3.1. Region of Interest of in a thermal image

To divide the dataset, the normalized histogram of the image is selected as a feature and k-means clustering is applied to divide the images into clusters. However, the histogram of the entire image indicates a large amount of black pixels, because the thermal camera is focused for approximately 37°C and the temperature of the background is lower, hence the pixels out of the silhouette of the patient are black. To consider only the distribution of the measured temperature of the patient, we apply a simple thresholding to extract the region of interest of the image. The applied threshold is the 20% of the difference of the maximal and minimal temperature of the image and we eliminate the region under the neck to be able to focus only on the face region. The ROIs of some images of the investigated dataset can be seen in Figure 2.

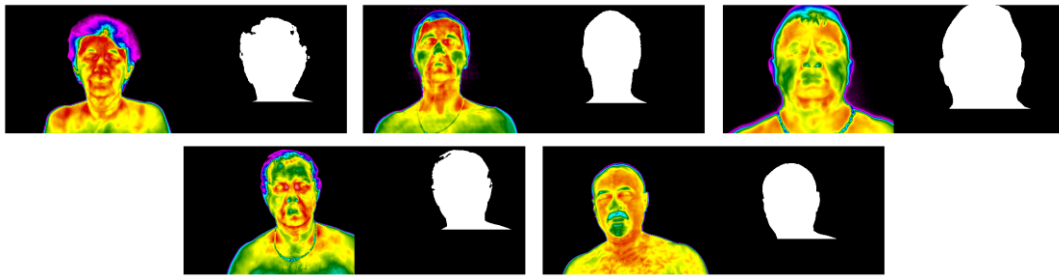


Fig. 2. Some input images and their regions of interest.

### 3.2. Features for clustering

When the examination is performed, the patients are not at the same distance from the thermal camera, hence the number of the pixels in the ROI varies. For compensation, we consider the normalized histogram of the ROI, which contains the relative frequency of the intensities:

$$H_i = \frac{h_i}{\sum h_i},$$

where  $h_i$  is the  $i^{th}$  bin of the histogram, while  $H_i$  is the  $i^{th}$  bin of the normalized histogram.

We analyze 8-bit grayscale images, hence we extract a 256-bin normalized histogram from each image, which is used as a feature vector in the classification process:

$$f^l = (H_0, H_1, \dots, H_{255}).$$

### 3.3. Image clustering

To determine the optimal number of clusters we used k-means clustering and validity indices [4-8] as cluster validation techniques which are based on intra and inter-cluster densities. Thus, our image dataset which contains 40 thermal images about patients are divided into training and test sets. This dataset was collected by a private ophthalmology clinic. We cluster the training image into  $1 \leq k \leq M$  clusters according to the distance of the images and each clustering is evaluated according to the following indices which are maximized or minimized when image clustering is optimal. To measure the distance between images Euclidean distance is used: given  $I_1$  and  $I_2$  with corresponding feature vectors  $f^{I_1}$  and  $f^{I_2}$ , the distance of these images is calculated in the following way:

$$d(I_1, I_2) = (f^{I_1} - f^{I_2}) \cdot (f^{I_1} - f^{I_2})'.$$

#### 3.3.1. Calinski-Harabasz index

For each number of clusters  $k \geq 2$ , the Calinski-Harabasz index [5] is defined as follows:

$$Calinski - Harabasz_k = \frac{tr B_k / (k - 1)}{tr W_k / (n_i - k)},$$

where  $B_k$  and  $W_k$  are the pooled between- and within-group covariance matrices for any given partition of the sample given  $k$ , respectively.  $tr$  denotes the sum of the diagonal entries,  $n_i$  is the size of cluster  $i = 1, \dots, k$ . This index is maximized, when  $k$  is equal to the optimal number of clusters.

#### 3.3.2. Krzanowski-Lai index

For each number of clusters  $k \geq 2$ , the Krzanowski-Lai [6] index is defined in the following way:

$$diff_k = (k - 1)^{2/p} \cdot tr \cdot W_{k-1} - k^{2/p} \cdot tr \cdot W_k,$$

$$Krzanowski - Lai_k = \frac{|diff_k|}{|diff_{k+1}|},$$

where  $W_k$  is the within-group covariance matrix and  $tr$  denotes the sum of the diagonal entries same as prior definition and suppose that  $p$  variables have been measured on each of the  $N$  sample objects. The optimal number of clusters is equal to  $\text{argmax}_{k \geq 2} (Krzanowski - Lai_k)$ .

#### 3.3.3. Dunn's index

The Dunn's validity index [7] is defined as follows:

$$Dunn = \min_{1 \leq i \leq k} \left\{ \min_{\substack{1 \leq j \leq k \\ j \neq i}} \left\{ \frac{\delta(X_i, X_j)}{\max_{1 \leq c \leq k} \{\Delta(X_c)\}} \right\} \right\},$$

$$\delta(X_i, X_j) = \min_{x \in X_i, y \in X_j} \{d(x, y)\},$$

$$\Delta(X_c) = \max_{x, y \in X_c} \{d(x, y)\},$$

where  $X_i$  represents the  $i^{th}$  cluster of a clustering,  $\delta(X_i, X_j)$  defines the distance between clusters  $X_i$  and  $X_j$  (intercluster distance),  $\Delta(X_c)$  represents the intracluster distance of  $X_c$ , and  $k$  is the number of the clusters of a partition. The optimal number of clusters maximizes the *Dunn* index, because the intercluster distances are maximized and the intracluster distances are minimized.

### 3.3.4. C-index

The C-index [8] is defined as:

$$C - index = \frac{S - S_{min}}{S_{max} - S_{min}},$$

where  $S$  is the sum of distances over all pairs of images from the same cluster and  $t$  is the number of these pairs. Let  $T$  be the number of all possible pair of images in the training set. After ordering the  $T$  pairs according to their distance, we select the  $t$  smallest and the  $t$  largest pairs. Then  $S_{min}$  is the sum of the  $t$  smallest distances and  $S_{max}$  is the sum of the  $t$  largest distance. The optimal number of clusters minimizes the *C - index*.

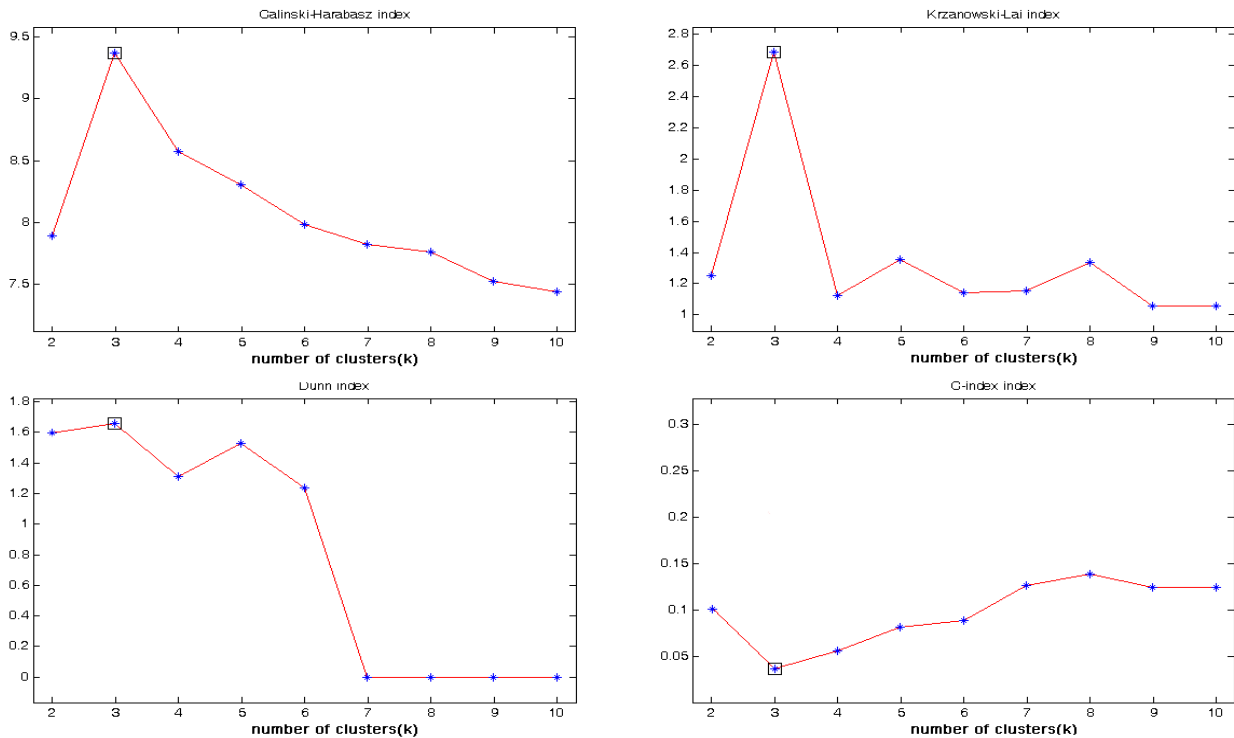


Fig. 3. Optimal number of clusters found by the indices are marked with squares.

After the calculation of these indices, we found that the optimal number of clusters is three for our dataset as can be seen in Figure 3. The resulting clusters are different regarding the temperature behavior of the images. The first cluster contains images with lower temperature, mainly normal images. The images in the second cluster show high similarity to each other (both normal and abnormal). The third cluster contains images with higher temperature, mainly abnormal images. Figure 4 shows the result of the clustering for the training dataset.

For each cluster an optimal parameter setting is determined using simulated annealing [9]. For the test images the normalized histogram is created as described above, the image is assigned to the closest cluster and the optimal parameter setting of this cluster is applied.

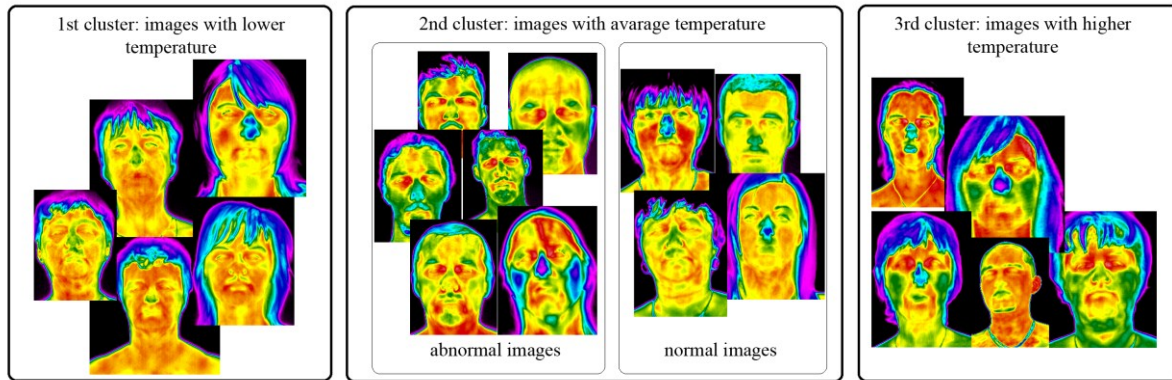


Fig. 4. The result of the clustering: clusters with different temperature behavior.

#### 4. Specification of SVM parameters

To take advantage of the above clustering step, we have determined specific parameter settings for the SVM classifier for each cluster. That is, we determine the optimal parameters for each cluster and an input image is labeled by optimal adjusted SVM regarding the closest cluster of the input image. Since the accuracy of the classification depends on the feature set, the kernel function and the method for finding separating hyper-plane of SVM and this parameter space is rather large. Thus, we used a stochastic search algorithm (simulated annealing again) to select the most appropriate adjustment of SVM for each cluster.

To perform the simulated annealing and the evaluation of our method, we needed an image set which contains manually labeled images by a clinical expert. Our image set contains 20 normal and 20 abnormal images which are not completely sufficient to an exhausting testing. So after the optimal parameters were determined, to measure the performance of the proposed method we evaluated the performance of simulated annealing by a cross-validation technique. That is, we randomly selected images for the training and test set which contained both normal and abnormal images with known label. Then, we divided the training images into three disjoint clusters, assigned a closest cluster based on a simple nearest-neighbor search to each test image and performed simulated annealing. All these steps were repeated for 100 times to get valid parameter settings.

In each iteration, the simulated annealing algorithm determines the optimal parameter setting of the SVM for each cluster by minimizing the following energy function:

$$f_{energy} = -1 \cdot sensitivity \cdot specificity,$$

$$sensitivity = \frac{true\ positive}{true\ positive + false\ neagtive},$$

$$specificity = \frac{true\ negative}{true\ negative + false\ positive}$$

After the simulated annealing determined the optimal parameters for each cluster by 100 times, we select those parameter settings for the clusters which are advised most frequently with a lowest energy function value. According to this selection we found the following feature set and parameters to train the SVM for the three clusters.

Table 1. Optimal parameter settings for individual clusters.

	First Cluster	Second Cluster	Third Cluster
Kernel function for data mapping into kernel space	Linear kernel	Quadratic kernel	Linear kernel
Method for finding separating hyper-plane	Quadratic Programming	Least Square	Quadratic Programming
Proposed feature subset for classification	entropy, skewness, kurtosis of histogram and entropy, correlation of co-occurrence matrix in all of 4 direction of undivided regions of left and right eye	entropy, skewness, kurtosis of histogram and entropy, energy, homogeneity, correlation of co-occurrence matrix in all of 4 direction of undivided regions of left and right eye	entropy, skewness, kurtosis of histogram and entropy, correlation of co-occurrence matrix in all of 4 direction of undivided regions of left and right eye

## 5. Experimental Results

We determined the appropriate setting of the SVM for each cluster and we evaluated the performance of the proposed method. The test is performed analogous to the way how the optimal parameters are determined. That is, we applied cross-validation for setting up the training and the test sets. In 100 iteration, we randomly selected the images for the training set, we applied k-means clustering to divide them into three cluster as can be seen in Figure 4. Then, the SVM is trained on each cluster individually with the corresponding parameter setting. Rest part of the image set is considered as test set and each image is assigned to the closest cluster based on the Euclidean distance of the images. Regarding the closest cluster, each test image is labeled by the adequate SVM classifier.

Our experimental results can be found in Table 2, where the percentage value shows the average accuracy of the responses of the SVM for input images in the 100 iteration. Accuracy is the ratio of the correctly labeled images regarding the total number of input images. For the sake of completeness, we also disclose the sensitivity and specificity values.

As it can be seen from the results, we have achieved higher accuracy as if we apply the same SVM parameter setting to each image. Also note that the labels of the images which are assigned to the first or third clusters are almost completely correct and the clustering may be considered as pre-classification step.

**Table 2. Results of classification.**

	Accuracy	Sensitivity	Specificity
Result with no clustering [1]	78,9%	83,6	74,2
<b>Result with the proposed method</b>	<b>97,3%</b>	<b>0,99</b>	<b>0,95</b>

## 6. Conclusion

We proposed a method which can detect excessive activation of the ciliaris muscle in the human eye on thermal images with high accuracy. Image clusters are created based on a training dataset which contains manually labeled images by a clinical expert. Optimal parameter settings of an SVM classifier are determined for each image cluster by simulated annealing and the optimal adjusted SVM is trained separately to each cluster. We use the proper parameter setting on an unknown image as follows: the normalized histogram of the image is created, the closest cluster is assigned to the unknown image using k-NN classifier, and the optimal parameter setting of this cluster is applied for SVM, and the properly adjusted SVM classifies the image. Experimental results showed that the method is likely to be applied for the designated aim.

## REFERENCES

- [1] Harangi B., Csordás T., Hajdu A., "Detecting the Excessive Activation of the Ciliaris Muscle on Thermal Images", IEEE 9th International Symposium on Applied Machine Intelligence and Informatics (SAMII), 2011, pp. 329 – 331.
- [2] Diakides N. A., Bronzino J.D., "Medical Infrared Imaging", CRC Press Taylor & Francis Group, 2007.
- [3] Ng E.Y., Ung L.N., Ng F.C., Sim L.S., "Statistical analysis of healthy and malignant breast thermography", Journal of Medical Engineering and Technology, vol. 25, no. 6, pp. 253-263, 2001.
- [4] Bolshakova N., and Azuaje F., "Cluster Validation Techniques for Genome Expression Data", Signal Processing, vol. 83, no. 4, pp. 825-833, 2002.
- [5] Calinski R., Harabasz J., "A dendrite method for cluster analysis", Communications in Statistics - Theory and Methods, vol. 3, no. 1. pp. 1-27, 1974.
- [6] Krzanowski W., Lai Y., "A criterion for determining the number of groups in a dataset using sum of squares clustering", Biometrics vol. 44, no. 1, pp. 23-34, 1988.
- [7] Dunn J., "Well separated clusters and optimal fuzzy partitions", Journal of Cybernetics, vol. 4, no. 1, pp. 95-104, 1974.
- [8] Hubert L., Schultz J., "Quadratic assignment as a general data-analysis strategy", British Journal of Mathematical and Statistical Psychology, vol. 29, no. 2, pp. 190-241, 1976.
- [9] Kirkpatrick S., Gelatt C. D., and Vecchi M. P., "Optimization by simulated annealing", Science, vol. 220, no. 4598, pp. 671-680, 1983.